Journal of Controlled Release 170 (2013) 477–484

Contents lists available at SciVerse ScienceDirect

Journal of Controlled Release

journal homepage: www.elsevier.com/locate/jconrel

NANOMEDICINE

Can bioadhesive nanoparticles allow for more effective particle uptake from the small intestine?

J. Reineke [a,1], D.Y. Cho [b,1], Y.L. Dingle [b], P. Cheifetz [b], B. Laulicht [b], D. Lavin [b], S. Furtado [b], E. Mathiowitz [b,*]

[a] Department of Pharmaceutical Sciences, Eugene Applebaum College of Pharmacy and Health Sciences, Wayne State University, Detroit MI 48202, USA
[b] Department of Molecular Pharmacology, Physiology and Biotechnology, Brown University, Providence RI 02912, USA

ARTICLE INFO

Article history:
Received 23 January 2013
Accepted 31 May 2013
Available online 21 June 2013

Keywords:
Bioadhesion
Nanoparticles
Uptake
In-vitro in-vivo correlation

ABSTRACT

There has been increasing interest in developing bioadhesive nanoparticles due to their great potential as carriers for therapeutics in oral drug delivery systems. Despite decades of research, such a system still has not been successfully implemented. This paper demonstrates the enormous potential of such engineered systems: the incorporation of a bioadhesive coating, poly(butadiene-maleic anhydride-co-L-DOPA) (PBMAD), to non-bioadhesive nanospheres resulted in an enhancement of particle uptake in the small intestine from 5.8 ± 1.9% to 66.9 ± 12.9%. Direct correlation was obtained between bulk tensile strength, *in vitro* binding to everted intestinal sacs and quantitative *in vivo* uptake; this data suggests that bulk properties of polymers can be used to predict bioadhesive properties of nano- and microparticles. The differential distribution of the nanospheres to various tissues following uptake suggests surface chemistry plays a significant role in their localization within the body. The results of these studies provide strong support for the use of bioadhesive polymers to enhance nano- and micro-particle uptake from the small intestine for oral drug delivery.

© 2013 Elsevier B.V. All rights reserved.

1. Introduction

Micro- and nanosphere-based polymeric delivery systems have great potential for oral drug delivery due to their ability to protect encapsulated therapeutic agents from the harsh gastrointestinal tract and to allow for controlled drug release kinetics. Although a significant amount of effort has been focused on developing effective delivery systems for translation into clinical use, a major obstacle in the development of effective nanospheres for oral drug delivery is achieving high enough levels of uptake to reach therapeutic concentrations of the encapsulated drugs after administration. Thus, a variety of strategies have been evaluated for their potential to enhance the translocation of particles from the intestinal lumen, but most with limited success.

The phenomenon of bioadhesion or mucoadhesion, originally described by Park and Robinson, refers to the interactive forces between a synthetic or biological material and a mucosal surface [1]. When applied to oral drug delivery, bioadhesive polymers result in adhesion to the mucous membrane proximal to the intestinal cells allowing for enhanced interactions with the absorptive epithelium thereby increasing gastrointestinal transit time. There are several proposed mechanisms that mediate bioadhesion between the polymer and biological substrate; the most studied are mechanical and/or chemical interactions [1,2]. Mechanical bonds can be the result of the physical entanglement of mucin strands with polymer chains, as is the case for hydrogels, which are most often used for bioadhesive drug delivery [3,4]. Alternatively, chemical mechanisms can include strong primary bonds, which are not desired, as well as weaker secondary forces such as ionic bonds, Van der Waal's interactions and hydrogen bonds [3,5]. While the strengths of individual secondary forces are relatively weak, the high numbers of these interactions possible with polymeric materials can generate strong bioadhesion to mucus. Thus, polymers with high molecular weights and greater concentrations of reactive polar groups (−COOH, −OH) tend to develop more intense mucoadhesive bonds [2,5–11]. Studies have shown that thermoplastic polymers that are high in carboxyl groups can also produce intense bioadhesive interactions without physical entanglement [12–27] and be effective in improving the bioavailability of orally administered therapeutics [28,29].

Nanoparticles made of bioadhesive polymers may, therefore, potentiate effective oral drug delivery due to the combination of their small size and high surface area [30–34]. Many reports have shown that the surface chemistry greatly affects the uptake of particles [35–40], which could be of particular interest given the high surface area associated with nanoparticles. However, no systematic study has directly investigated the relationship between bioadhesive nanospheres and intestinal uptake of nano- or microparticles.

For the last decade, work in our laboratory has focused on developing quantitative *in vitro* [2,12,16–23,41] and *in vivo* [16,18,24–26] methods to measure bioadhesion between microspheres and intestinal mucosal tissue. As part of this research, we have identified a series of quantitative techniques that helped us evaluate, what we believe,

* Corresponding author at: Brown University, Box G Biomed Center, Providence, RI 02912, USA. Tel.: +1 401 863 1358; fax: +1 401 863 1753.
E-mail address: Edith_Mathiowitz@brown.edu (E. Mathiowitz).
[1] These authors contributed equally to this work.

0168-3659/$ – see front matter © 2013 Elsevier B.V. All rights reserved.
http://dx.doi.org/10.1016/j.jconrel.2013.05.043

to be the critical parameters to select effective bioadhesive polymers. We then have made nanoparticles from those characterized materials and revealed that the most adhesive materials exhibit substantial uptake *in vivo*. The initial evaluations were judged by optical, confocal and TEM microscopy. The results that have been published [21] are summarized schematically in the first three columns of Fig. 1. The data presents real measurements for fracture strength, contact angles and everted sac values, and only relative values for uptake as assessed by microscopy [21]. The data indicate strong correlation between all the methods used to evaluate bioadhesion in those four different polymers [21]. To be more specific, tensile work measurements of the bulk bioadhesive properties of the polymers polystyrene (PS; non-erodible) and poly(fumaric-co-sebacic) acid (P(FASA), bioerodible) exhibited the strongest mucoadhesive forces. Poly(lactic acid) (PLA) and poly(lactic-co-glycolic acid) (PLGA) exhibited weaker mucoadhesive forces. Studies of the contact angle which are also strong indicators for bioadhesion, revealed that both PS and P(FASA) had a high contact angle with water, indicating low affinity toward aqueous solution. In contrast, when contact angle was measured with mucus, it was clear that the first two polymers had the lowest contact angle with mucus indicating strong affinity for mucus [1,21]. This was further confirmed by additional measurements using an *ex vivo* everted sac assay, providing further evidence that the most adhesive polymers in the series to be PS and P(FASA) followed by PLGA then PLA. Interestingly, when we prepared nanospheres from each of these polymers and evaluated uptake qualitatively from the small intestine using optical, confocal and transmission electron microscopy we found that PS and P(FASA) nanoparticles revealed qualitatively high uptake while PLGA and PLA lagged behind [1,2,16,21,24]. The results of this prior work provide a series of important parameters that allow for the identification and evaluation of potential bioadhesive polymers for potential use in drug delivery applications. The most adhesive polymers are those with hydrophobic backbones and with high carboxylic end groups. [3,4,12,16–26,32,41]. While it is hard to monitor the uptake of biodegradable polymers *in vivo*, particularly P(FASA) that degrades extremely fast, it is easy to follow nondegradable polymers such as PS that will stay intact after potential uptake. For the current work we chose to work with non-degradable polymers, without any drug, since the work focuses on evaluating the potential of total uptake of the entire nano- or microparticles. Since PS, as well as PMMA, are non-erodible polymers, they can be used to advance our previous studies by quantitatively tracking the fate of nanoparticles after *in vivo* administration.

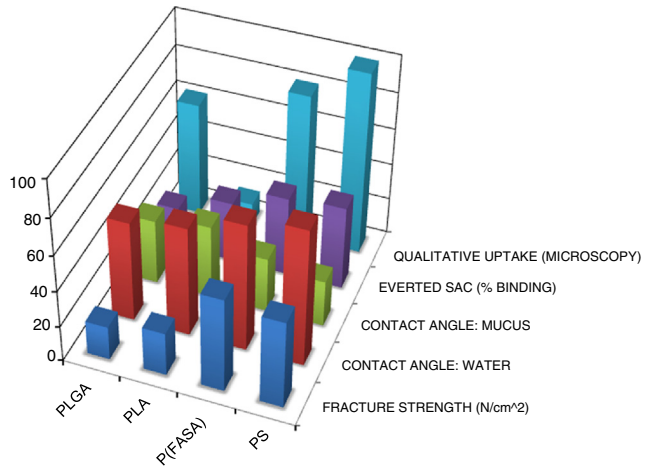

Fig. 1. 3-D representation of critical *in vitro* and *in vivo* bioadhesion parameters for PLGA, PLA, P(FASA) and PS. Qualitative uptake value is based on microscopy counts of nanoparticle uptake from representative histological samples and normalized to the number PS nanoparticle uptake [2,3,5–11,21,24].

Thus, the current study was directed to quantify the exact uptake of polymeric nanoparticles *in vivo* (without any drug) using an isolated loop technique and to evaluate the role of our most adhesive polymer, poly(butadiene-maleic anhydride-co-L-DOPA) (PBMAD) [12–27] on nanoparticle uptake and tissue distribution. To address this question we chose two different nanosphere formulations made of non-erodible polymers and characterized the tensile bioadhesive forces of the bulk polymer and the amount binding to everted intestinal sacs. The less adhesive formulation was coated with PBMAD and uptake and biodistribution of all three formulations were evaluated in the small intestine.

2. Materials and methods

2.1. Materials

Polystyrene beads (500 nm) were purchased from Polysciences, Inc. (Warrington, PA) and stored at 4 °C until use. Suspensions were used as supplied in concentrations of 25 mg/ml. Polymethyl methacrylate (PMMA; MW = 100 kDa) and polyvinyl alcohol (MW = 25 kDA, 88% hydrolyzed) were purchased from Polysciences, Inc. (Warrington, PA) and stored at room temperature.

2.1.1. Synthesis of PBMAD

Poly(butadiene-maleic anhydride-co-L-DOPA) (PBMAD), was synthesized as described by [20,28,29]. Briefly, the PBMAD is prepared using commercially available poly(butadiene-maleic anhydride) (MW = 10,000–15,000 Da) through the ring opening of the maleic anhydride via hydrolysis to maleic acid followed by the subsequent conjugation of L-DOPA to these newly formed carboxyl groups via an amide bond. The polymer synthesis yield was ~50–60% [20,30–34]. FTIR and DSC confirmed the successful side-chain grafting of the amino acid and further analysis with NMR revealed a 75% grafting efficiency. The details of the synthesis and characterization of this polymer are described in [20,35–40]. All solvents were of the highest commercial grade available.

2.2. Preparation of PMMA microspheres by solvent evaporation

The PMMA is a linear polymer and thus, the solvent evaporation technique was used to prepare the nanospheres; the process was performed at room temperature and without the need for cross-linking. PMMA was dissolved in chloroform at a concentration of 3.3% w/v to comprise the organic phase. An aqueous phase of 1% w/v polyvinyl alcohol (25 kDa, 88% hydrolyzed) was prepared and mixed under a VirTis Cyclone IQ2 SENTRY microprocessor at 25,000 rpm with a straight open blade and VirTis baffled homogenizer flask. The organic phase with polymer was then added to the aqueous phase forming an o/w emulsion and continually mixed for 15 min. The emulsion was then added to a 1% w/v polyvinyl alcohol (25 kDa, 88% hydrolyzed) bath and mixed under an over-head stirrer for 12 h at 3000 rpm to allow further evaporation and curing. This suspension was then centrifuged at 4000 rpm for 20 min and the supernatant poured off. The pellet was resuspended and washed in deionized water three times. Finally, the formulation was lyophilized for 48 h and stored as a dry powder at room temperature until use. The desired particle size range was obtained through the optimization of the shear rate during the emulsification step of nanosphere preparation. The freeze-drying process leaves minimal concentrations of chloroform in the spheres and no cytotoxic effect of residual solvent in nanospheres prepared using this method were observed in *in vitro* cell culture models.

2.3. Preparation of coated PMMA nanospheres using phase inversion nanoencapsulation

A modified version of phase inversion nanoencapsulation, originally described by Mathiowitz et al. [2,12,16–23,27,41], was utilized

to fabricate spheres consisting of PMMA and PBMAD. First, PMMA was dissolved in 5 ml of tetrahydrofuran (2% w/v) and, in a separate vial, PBMAD was dissolved in 10 ml of ethanol (2% w/v). The polymer solutions were mixed resulting in a precipitation of the PMMA only, in the presence of the ethanol. The PMMA suspension with dissolved PBMAD is then rapidly added to a non-solvent bath of petroleum ether thus precipitating the PBMAD around the PMMA. As a result of this two-step precipitation, the PBMAD is likely coating the PMMA, but there is likely heterogeneity in the nanoparticles as well. Nanospheres were collected by positive-pressure filtration through PTFE filter paper with a pore diameter of 0.2 μm and lyophilized for 48 h. Formulations were stored under vacuum-seal at room temperature until use. As described in our previous work, particle size is a function of polymer solution viscosity; thus, the polymer solution concentrations were optimized for the formation of particles of the desired size range.

2.4. Evaluation of microspheres by scanning electron microscopy

Morphology and particle size of formulations fabricated by solvent evaporation and phase inversion nanoencapsulation were analyzed by scanning electron microscopy. Formulations in dry powder form were placed on a carbon-backed adhesive and sputter-coated with Au–Pd for 4 min at 20 mA and imaged on a Hitachi 2700 with an accelerating voltage of 8 kV.

2.5. Particle size analysis of microspheres

Solvent removal and phase inversion nanoencapsulation formulations were reconstituted from powder form into an aqueous solution using 1% w/v sodium lauryl sulfate (SLS)/1% w/v polyvinylpyrrolidone (PVP) reconstitution media and bath sonication in 0.5–2% w/v suspensions. Polystyrene nanosphere suspensions were diluted with deionized water down to ~1% w/v solutions from the original supplied suspensions. A Beckman Coulter LS230 Laser Diffraction Particle Size Analyzer was used to evaluate size and size distribution of nanoparticle populations.

2.6. Characterization of microspheres by light microscopy

All formulations were imaged with light microscopy to evaluate morphology and aggregation. Formulations were suspended in 1% w/v SLS/1% w/v PVP reconstitution media at a concentration of 0.5% w/v. Drops of the suspension were placed on a slide and sealed under a cover slip with fast-drying nail polish. Slides were then imaged on a Zeiss Axiovert 200 M microscope. To obtain bright field images a 40× water objective was used along with DIC and phase contrast techniques. Images were taken with a Zeiss AxioCam MRc5 digital color CCD camera. We selected the largest particle in the field (about 5 μm) to demonstrate the coating of one layer by another.

2.7. Determination of PMMA content in the PBMAD/PMMA formulation

To determine the weight percent of PMMA in the PBMAD/PMMA formulation fabricated by phase inversion nanoencapsulation, an extraction and chromatography detection method was used. First, a known amount (25–50 mg) of the PBMAD/PMMA formulation was weighed into a vial and 5 ml of chloroform was added. The solution was mixed on an end-over-end mixer for 1 h to ensure complete dissolution of PMMA into the chloroform. Then, a 1 ml sample of the PMMA solution was filtered through a 0.2 μm PTFE syringe filter into a sample vial for gel permeation chromatography. The sample elution time of extracted PMMA was detected on a Shimadzu RID-10A refractive index detector after flow (1 ml/min) through a column bank consisting of Waters Styragel HR4E and HR5E columns. The area under the distinctive PMMA peak on the refractive index versus elution time graph was calculated using Shimadzu software and compared to a linear standard curve of PMMA to directly yield the quantity of PMMA in the PBMAD/PMMA formulation.

2.8. Bioadhesion measurements using texture analyzer

Testing the bioadhesion of bulk polymeric materials to *ex vivo* rat jejunum was performed with a TA.XTplus Texture Analyzer (Texture Technologies Corp., Scarsdale, NY) equipped with a 1 kg load cell with 0.2 g sensitivity. Glass-headed pins with mean head diameter ~2.8 mm were dip-coated into various 5% w/v solutions of each polymer (PMMA and PS in methylene chloride, PBMAD in acetone) and dried between coatings to achieve a uniform coating around the pinhead; the pins were dipped 8 times to ensure an adequate amount of polymer was coated onto each pin. Individual probes were then fitted onto the texture analyzer load arm and a biological sample chamber placed on the stage containing freshly excised rat jejunum submerged in phosphate buffer saline, pH 7.4 with luminal side facing upward at 37 °C. The load arm descended at 0.5 mm/s until a specified target force (5 g) between the sample probe and intestinal tissue was reached. This position was then held for 7 min (as has been optimized by our group to allow for polymer hydration and the generation of bioadhesive interactions with the small intestinal tissue) [16–18,20,22–26] followed by a rising of the load arm at 0.5 mm/s. In addition, to study the effect of adding surfactants that will be later used to administer the microsphere, we evaluated the same adhesive forces with all polymers in the present of 1% SLS and 1% PVP in the media. No change was observed in adhesive forces as a result of these surfactants.

Fracture strength was determined by taking the peak tensile load (found at the beginning of the fracture) and normalizing this value for the projected surface area (PSA) of the probe. Calculation of PSA by the relation $PSA = \pi(r^2 - [r - a]^2)$ where r is the radius of the sphere as measured by calipers and a is the depth of penetration. Tensile work was determined by taking the area under the fracture curve and normalizing for PSA.

2.9. Everted sac bioadhesion assay

Utilizing an everted sac assay modified from Santos et al. [17,21] the relative bioadhesion for each nanosphere formulation was determined. Male, Sprague–Dawley rats weighing 200–250 g were anesthetized with 3% isoflurane prior to a midline abdominal incision. The jejunum was removed, flushed with PBSG, and immediately immersed in fresh PBSG. Segments of jejunum, 6 cm in length, were everted, using a stainless steel rod, and ligated at both ends with silk 0–0 monofilament sutures. The everted sac was then filled with ~2 ml PBSG (pH 7.4) and immersed in a nanosphere suspension prepared as follows. Pre-warmed (37 °C) PBSG (pH 7.4) was added to 60 mg of formulation (0.4% w/v) and bath sonicated for 5 min. Once the isolated loop was added to the nanosphere suspensions, samples were placed on an end-over-end mixer at 37 °C for a 30-minute period, which allows for the maximal time for the nanoparticles to interact with the small intestinal tissue while maintaining viability [17,21]. During this incubation period nanospheres are allowed to adhere spontaneously to the everted intestinal loop. Following incubation, the everted sac was removed, gently rinsed and processed as two samples (the tissue loop with adhered nanospheres and the nanosphere suspension).

To quantify the amount of marker polymer (polystyrene or PMMA) in both the bound (everted sac tissue sample) and unbound (remaining nanosphere suspension) samples, gel permeation chromatography was used as described in further detail below. Results are presented as a binding ratio for each formulation with the binding ratio being defined as the ratio of the amount detected on the everted sac tissue to the amount detected in the suspended supernatant after removal of the everted sac tissue.

2.10. In vivo dosage preparation

Suspensions of nanosphere formulations were utilized for all *in vivo* experiments. Polystyrene nanospheres are supplied as a 2.5% w/v suspension and were used as received. For PMMA and PBMAD/PMMA formulations, the powder formulation was added to 1% SLS/1% w/v PVP to a final concentration of 2.5% w/v. To adequately disperse the formulations, solutions were bath sonicated for 10 min immediately before administration. A dosage volume of 1 ml was used in all studies and resulted in a total dose of 25 mg.

2.11. In vivo isolated loop particle uptake experiments

For a controlled, direct administration of formulations to a specific gastro-intestinal region, an isolated loop technique was employed. Male, Sprague–Dawley rats, weighing 200–250 g were allowed access to standard chow and water ad libitum. Rats were anesthetized with 3% isoflurane inhalation. A 6 cm intestinal length was isolated by suture ligation with monofilament silk 0–0 sutures at each end taking care not to disrupt blood flow from mesenteric arteries. Suspensions of the nanospheres were then injected directly into the isolated region's lumen. The isolated loop was returned to the abdomen, which was then closed to maintain body temperature and moisture. Following a 5 hour incubation period, the following samples were collected in order: 1 ml of blood from the portal vein, 1 ml of blood from the celiac artery, lungs, heart, spleen, kidneys, liver, isolated loop, rinse of isolated loop, and brain. The 5-hour time point was selected based on previous experience from our research group with PS nanoparticle uptake studies and is the optimal point for investigation of nanoparticle uptake. All tissues were stored at −18 °C until further processing. Studies were run in animal cohort groups of 4 ($n = 4$) for each study.

2.12. Tissue processing and polymer detection

All samples from everted sac bioadhesion analysis and *in vivo* isolated loop experiments were processed and quantitatively analyzed for polymer content by gel permeation chromatography (GPC) as described herein. Nanospheres are comprised of nondegradable materials and the following methodology extracts intact nanospheres from samples for polymer detection. Tissue samples were physically cut into small pieces, added to ~5 ml PBS and homogenized on a Cole-Palmer Ultrasonic Homogenizer CV26 with a high gain Q horn and extender set at 40% amplitude for 30 s. Homogenized samples were then lyophilized for 48 h resulting in a powdered tissue digest. An extraction of the marker polymer was then performed by the addition of chloroform and mixing on an end-over-end mixer for 96 h. Extractions were then filtered through PTFE filters of 0.2 μm pore diameter to remove non-soluble debris. Filtered extractions were lyophilized for 24 h and stored at −18 °C until analysis.

Lyophilized extractions were reconstituted in 1 ml of chloroform by mixing on an end-over-end mixer for 1 h. The solution was filtered a final time through a 0.1 μm PTFE syringe filter and ran on a Shimadzu GPC equipped with Waters Styragel HR5E and HR4E columns and a Shimadzu RID-10A refractive index detector.

A specific peak for the marker polymer is identified and the area under the curve is calculated and related to the polymer concentration by comparison to a linear standard curve for PS and PMMA with R^2 values of 0.9993 and 0.9998, respectively. The PS curve was used for determining the content of PS using the tissue extracts while the PMMA curve was used to determine the tissue content of the PMMA studies; the PMMA loading of the double-walled formulation was used in conjunction with the PMMA standard curve for the PBMAD/PMMA studies. Sensitivity of the assay was tested over a range of 0.05 mg/ml to 25 mg/ml from doped tissue extracts. The linear relationship existed over the range of 0.2 mg/ml to 25 mg/ml. Below 0.8 mg/ml, peaks had to be manually selected as they were below the peak detection threshold of the software. Since the sample volume is known, the exact mass of polymer can be calculated from the detected concentrations. The uptake values were calculated using the amount of polymer detected in the tissues, which represents nanoparticles that have been taken up by the small intestine and distributed systemically. Residual nanospheres in the isolated loop lumen as well as particles attached to the isolated loop tissue were not included in the fraction of particles that have undergone uptake. Only the particles that have been taken up and translocated from the intestinal lumen to the circulation then distributed throughout the tissue have been considered in the determining uptake; thus, the uptake data in the manuscript are a strong indication of particle uptake.

The resulting data was computed to yield quantitative information regarding the uptake and tissue distribution by the following calculations. Percent uptake was calculated by taking the sum of all amounts detected in tissues (excluding isolated loop and loop rinse samples) divided by the total dose administered and multiplied by 100. Tissue distribution could be directly compared for each tissue across study groups. However, further information may be gained by comparison of each tissue across study groups after normalizing for uptake. Mass balance was determined as the sum of all amounts detected in tissues, isolated loop and loop rinse samples divided by the total administered dose. Mass balance values of 49.54 ± 0.78%, 102.96 ± 7.78% and 111.34 ± 67.0% were found for the PMMA, PS and PBMAD experiments, respectively (see Supplement material).

2.13. Statistical analyses

Standard errors were calculated and a 1-way ANOVA was performed with Microcal Origin Graphical Software (Northampton, MA). Significance was determined at $p \leq 0.05$.

3. Results and discussion

The motivation to quantify the amount of particle uptake was the direct result of the work presented in Fig. 1 [21]. While the original work focused on biodegradable polymers, which are hard to detect *in vivo*, polystyrene is a material that seemed to have appropriate bioadhesive forces and high uptake as judged by microscopy. Commercially available PS nanospheres and non-bioadhesive PMMA nanospheres were used as model polymers. To create a highly bioadhesive formulation, non-adhesive PMMA nanoparticles were coated with PBMAD, which was selected due to the high amount of carboxylic groups exposed on each side group (Fig. S3) which results in high bioadhesive properties and unique pH-dependent solubility in the gastrointestinal environment [18]. The polymer is stable at low pH and dissolves at high pH (above pH 8). Adhesion measurements of the bulk materials were compared to the everted sac measurements of each nanosphere formulation followed by quantification of the total uptake and biodistribution of the nanospheres after direct injection into isolated intestinal loops of rats *in vivo*.

The fabrication of the coated microsphere was done by phase inversion nanoencapsulation [16,27]. The process involves two steps of controlled precipitation: First, PMMA is dissolved tetrahydrofuran and PBMAD is dissolved in ethanol. The solvents are chosen such that once the polymer solutions are mixed PMMA precipitates due to the presence of the ethanol solution while the PBMAD is still soluble. The suspension (with dissolved PBMAD) is then rapidly added to a non-solvent bath of petroleum ether, which forces the precipitation of the PBMAD around the PMMA. As a result of this two-step precipitation, the PBMAD is likely coating the PMMA, but there is likely heterogeneity in the nanoparticles as well [36]. The PMMA loading results showed that 29.7% of the components are PMMA in the PBMAD/PMMA nanospheres composition. PMMA and PBMAD/PMMA nanospheres were spherical with a smooth external surface

morphology. SEM images of each formulation are shown in Fig. 2A–C. Average diameters of the formulated PMMA and PBMAD/PMMA nanospheres, as measured by laser diffraction, are 490 ± 550 and 540 ± 650 nm, respectively, and the purchased PS nanosphers are 540 ± 80 nm PS nanospheres. Volume average size distribution profiles of PS, PMMA and PBMAD/PMMA nanospheres are shown in Fig. 2D. The polydispersity of the formulated PMMA and PMMA/PBMAD nanospheres is much higher than the purchased PS nanoparticles and is considered in the interpretation of subsequent uptake results below. Electron microscopy has shown that the second larger peak in the size distribution profiles observed with the PBMAD/PMMA formulation is the result of aggregation due to the adhesive nature of the PBMAD.

Imaging with light microscopy showed a well-dispersed population of PMMA nanospheres (Fig. 2E) that appear translucent (Fig. 2e). PBMAD/PMMA nanospheres had a tendency to aggregate into irregular clumps when in solution (Fig. 2F) and appear yellow-brown due to optical properties of PBMAD. One large bead that was imaged under high magnification (Fig. 2f), depicts the yellow-brown colored PBMAD coating the clear PMMA core. FTIR of the raw materials of PMMA and PBMAD and the PBMAD/PMMA formulation (Fig. S1) confirm that both polymers are present in the final formulation while DSC analysis (Fig. S2) confirmed the phase separation of the two polymers in the formulation.

Bioadhesive measurements were performed on both the bulk materials and all nanosphere formulations. Adhesion measurements of the bulk materials, performed with a Texture Analyzer probe on freshly excised rat intestinal tissue, yielded statistically significant results for PMMA and PS, but PBMAD had a significant increase in bioadhesion both in terms of fracture strength (103.6 ± 8.3, 193.1 ± 31.4 and 242.6 ± 21.2 mN/cm^2, respectively), as shown in Fig. 3A, and tensile work (0.327 ± 0.09, 309.3 ± 28.6 and 20445.0 ± 5733.5 nJ, respectively). Texture analyzer bioadhesion studies were repeated for all three polymers in the presence of 1% SLS/1% PVP on freshly excised rat small intestinal tissue and revealed no difference in the bioadhesive forces measured compared to those discussed above (Fig. S4). Therefore, the presence of the surfactant, used for the dispersion of nanospheres for the subsequent everted sac and isolated loop studies, likely has minimal impact on the bioadhesion of the nanospheres to the intestinal tissue.

Bioadhesion of the nanosphere formulations was directly measured with the use of an everted sac technique with rat intestinal sections followed by quantitative extraction of nanospheres and GPC analysis. GPC analysis of the PBMAD/PMMA nanospheres showed that 29.7% of the composition is PMMA; thus, this data was used to determine the amount of the PBMAD/PMMA formulations detected in the tissue samples. Results are shown as a binding ratio (amount adhered to tissue:amount remaining in suspension) in Fig. 3B for PS, PMMA and PBMAD/PMMA nanospheres. PMMA nanospheres had the lowest bioadhesion with a binding ratio of 1.49 ± 0.82, followed by PS nanospheres with a binding ratio of 2.51 ± 0.40 and PBMAD/PMMA nanospheres had the highest bioadhesion with a binding ratio of 3.67 ± 2.38. There was an increase in bioadhesion of the PBMAD/PMMA nanospheres over the PMMA nanospheres with PS having an intermediate level of bioadhesion. The everted sac technique is useful in measuring the bioadhesion of the actual nanosphere formulations without an external force being applied; however, the variation with this method was high.

Comparison of the everted sac data for the bioadhesion of the nanospheres to the texture analyzer data for the bioadhesion of the bulk polymer revealed a strong direct correlation ($R^2 = 0.9608$) suggesting that the bioadhesive properties of the bulk polymer can

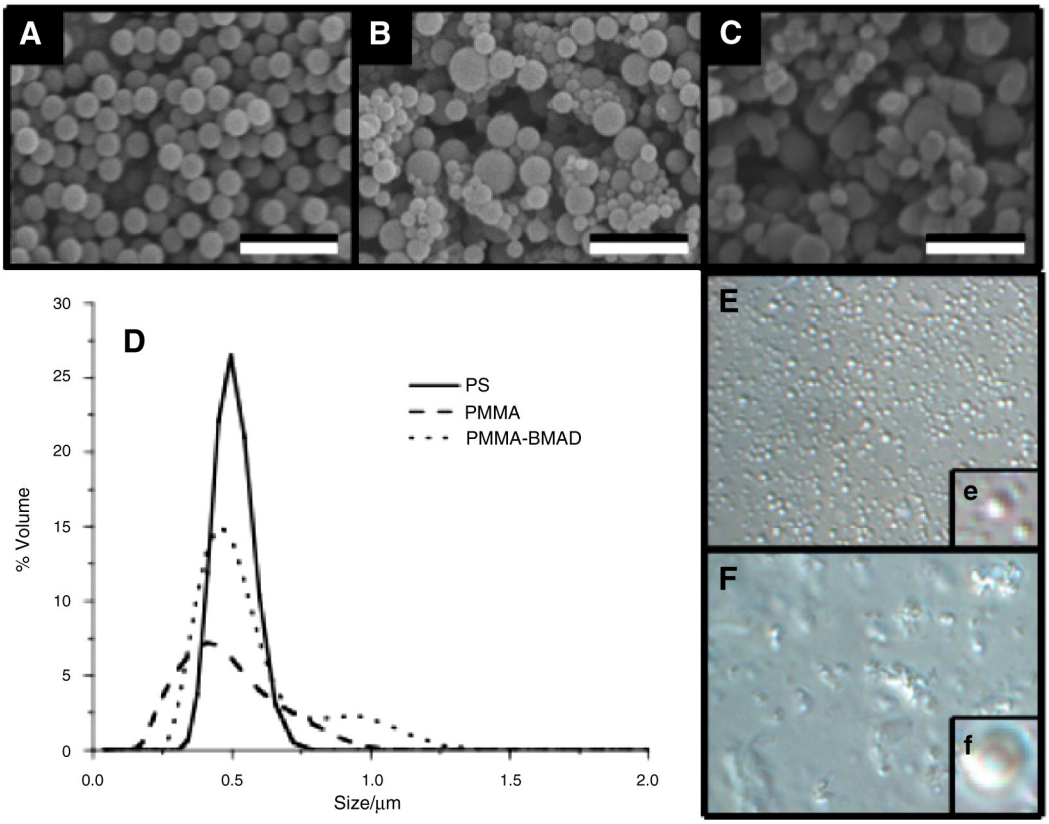

Fig. 2. Scanning electron microscopy of PS (A), PMMA (B), and PBMAD/PMMA (C) nanospheres. Scale bars = 2.0 μm. Size distribution profiles for each formulation as measured by laser diffraction are also shown (D). Optical microscopy of PMMA (E, e) and PBMAD/PMMA (F, f). Large sphere approximately 5 μm 40× (upper case) and 120× (lower case) magnification showing the coating on a single bead.

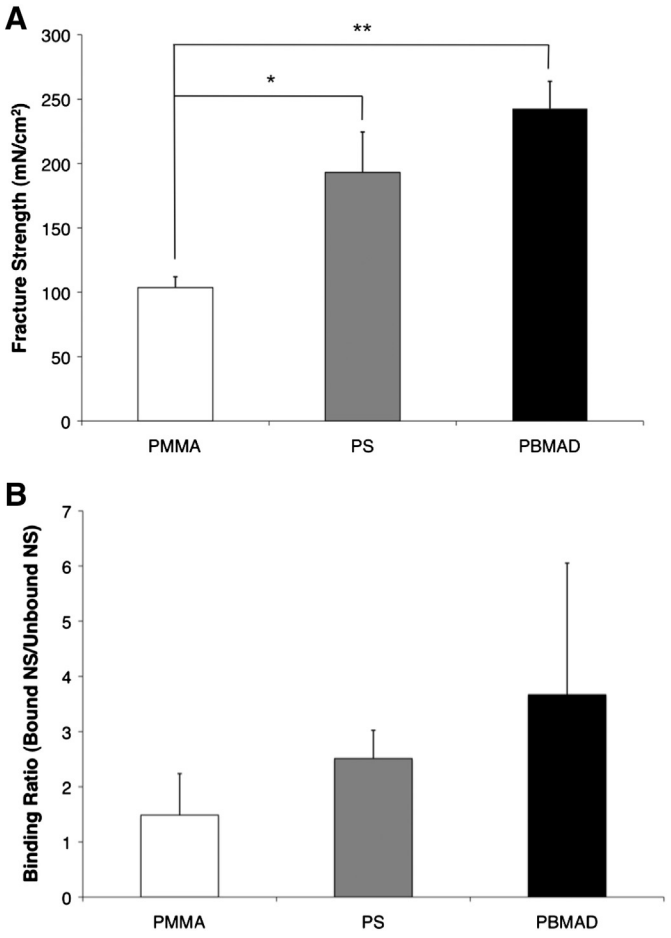

Fig. 3. (A) *In vitro* bioadhesion: Texture analyzer bioadhesion testing of bulk polymers: fracture strength of polymer probes with jejunum (n = 6), *p < 0.05, **p < 0.01; (B) *ex vivo* bioadhesion: Everted sac assay using 500 nm nanospheres with the small intestines of rats (n = 6).

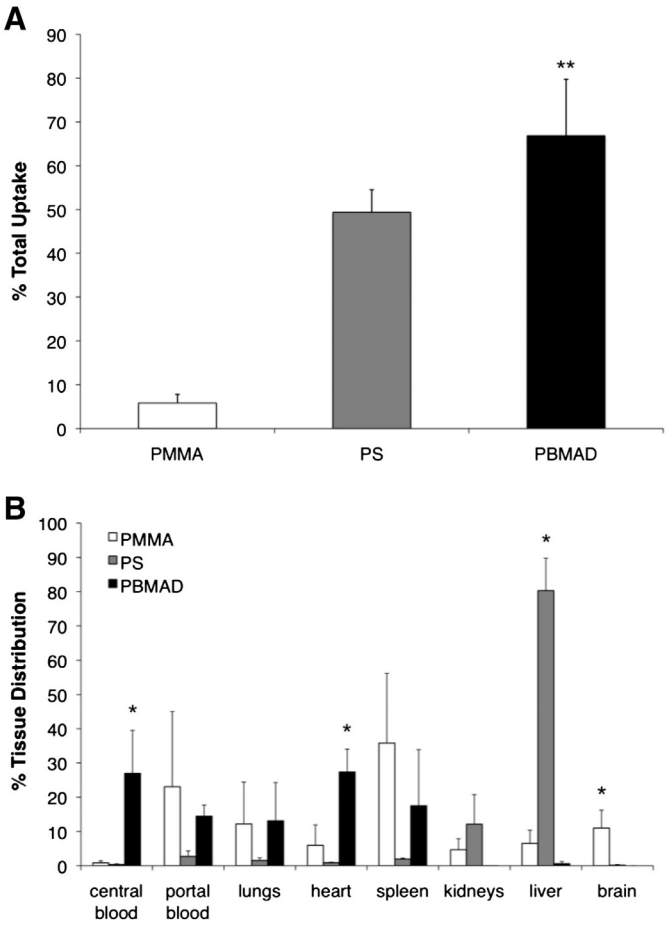

Fig. 4. (A) *In vivo* uptake: Total uptake of 500 nm nanospheres from isolated loop uptake studies in the jejunum (n = 6), **p < 0.01; (B) biodistribution: % tissue distribution of translocated 500 nm nanospheres following administration to the jejunum via isolated loop uptake study (n = 6), *p < 0.05.

be used to predict bioadhesive behavior on the nanoscale for these formulations and vice versa. The experiments were designed to ensure at least similar average diameters of the different formulations so that differences in bioadhesion are likely the predominant factor in uptake. The enhanced bioadhesion of the PBMAD/PMMA nanospheres is the result of the increased hydrogen bonding potential of the PBMAD polymer relative to the PMMA and PS, which allows for increased interactions with the mucin in the small intestine. Additionally, the PBMAD has unique characteristics that make it favorable for use in bioadhesive oral drug delivery applications. The chemical structure of the PBMAD dictates that the polymer is in its insoluble non-bioadhesive state at low pH environments, such as the stomach. However, upon exposure to more alkaline environments, like the small intestine, the polymer begins to solubilize and allow for bioadhesive interactions for more effective uptake of the carrier [20].

Delivering 500 nm PS, PMMA and PBMAD/PMMA nanospheres locally to the rat jejunum for a 5-hour period resulted in uptake of 45.8 ± 8.6%, 5.8 ± 1.9% and 66.9 ± 12.9% of the administered dose, respectively (Fig. 4A). Most surprisingly, by adding a bioadhesive PBMAD coating to the PMMA nanospheres, the uptake of these nanoparticles from the jejunum was increased substantially from 5.8 ± 1.9% to 66.9 ± 12.9%, a significant improvement over the non-bioadhesive PMMA formulation. It is previously noted that the formulated nanoparticles have a high size distribution relative to the purchased PS nanoparticles. It is shown in Fig. 2D that the PMMA/PBMAD nanoparticles are characterized with a slightly larger size distribution than the other formulations. Despite the growing literature indicating an inverse size relationship of nanoparticle size to cellular uptake [37,39,42,43], the bioadhesive nanoparticles still had higher uptake. We are unable to separate the nanoparticles of PMMA that were not coated with the PBMAD polymer, thus additional experiments were conducted in which PMMA microspheres were physically mixed with the bioadhesive polymer and administered under the same condition. The same enhanced uptake was obtained as seen with the coated nanoparticle, but with a much higher variability/standard deviation (See Fig. S5). Therefore, the high uptake is due to the presence of PBMAD polymer and nanoparticle coating likely ensures a higher percentage of uptake. Given this data we also postulate that the majority of the nanoparticles in the coated formulation are indeed coated with the PMAD polymer. This provides strong evidence for the use of bioadhesive polymers as a means of enhancing particle uptake from the small intestine. This is significant not only due to the high amount of uptake of the bioadhesive nanospheres, but also because it occurred in jejunum tissue free of Peyer's patches. Therefore, uptake likely occurred via the absorptive epithelium comprising ~98% of the surface of the small intestine. The likely mechanisms involved are a current area of further investigation in our laboratory.

The organ distribution following nanosphere uptake of the 500 nm PMMA, PS and PBMAD/PMMA formulations differed by a great amount as is evident in Fig. 4B. The PS nanospheres distributed almost entirely to the liver with some evident in the kidneys as well. However, for PBMAD/PMMA nanospheres an insignificant amount distributed to the liver, but instead distributed to many other tissues. PBMAD/PMMA nanospheres had 27.4 ± 16.4, 27.0 ± 12.5, 17.5 ± 15.2 and

13.1 ± 10.3% of the total uptake distributed to the heart, central blood compartment, spleen and lungs, respectively. Despite both formulations being similar in average size and morphology, they had largely different biodistribution profiles. The varied surface chemistries could have resulted in the varied biodistribution profiles, and could lead to the potential of passive targeting of nanospheres from the oral route by altering the surface properties. However, the mechanisms involved in disparate organ fate as a result of the three polymers investigated cannot be determined from these studies. Determinations of such mechanisms are very complex due to the numerous biological factors that may be involved (e.g. surface protein absorption, cell interaction, cell transit mechanisms, polymer matrix dynamics/swelling in biological fluids, etc.) and this is an area of continued investigation.

It is evident from the uptake data that the bioadhesive formulation (PBMAD/PMMA nanospheres) resulted in a much higher amount of intestinal uptake. When considering the bioadhesion and uptake of the three materials tested (PMMA, relatively non-adhesive; PS, moderately adhesive due to hydrophobic interaction; PBMAD, highly bioadhesive due to hydrogen bonding) there is a direct correlation of bioadhesion to intestinal uptake. Although many research groups, including our own, have theorized the potential benefit of bioadhesive nanospheres in oral drug delivery, this is the first time that a quantitative study has directly related bioadhesion to nanosphere uptake. Comparison of the bioadhesion measurements to the total intestinal uptake showed a strong linear correlation regardless of whether the nanosphere formulations were measured ($R^2 = 0.9255$) or the bioadhesion of the bulk materials were measured ($R^2 = 0.9941$).

4. Conclusion

In summary, this work demonstrates the high potential of bioadhesive nanospheres for potential applications in the delivery of therapeutics via oral administration. Strong correlations of intestinal uptake to the bioadhesive propertiesy of the bulk material as well as the bioadhesive properties of the nanosphere formulations were reported. Furthermore, the strong correlation observed between the bioadhesion testing of the bulk polymer and the nanospheres suggests that effective methods of testing bioadhesive phenomena can provide insight into both the macro- and nanoscale behavior of bioadhesive polymers. Lastly, nanospheres of different surface chemistries (PMMA, PS and PMAD) were observed to distribute differently to organs following internalization and may allow for the passive targeting of oral nanosphere drug delivery systems. This finding is currently under further investigation by the authors.

While the work presented in this paper evaluated the role of bioadhesion on total uptake of nanoshperes we are aware of the importance of drug encapsulation that was not included in this study. Indeed the success of this type of work will strongly depend on encapsulation and loading of the drug within the delivery system, through the use of biodegradable polymers. The evaluation of drug bioavailability and bioavailability of the delivery systems are two factors that need to be evaluated separately. We have addressed the uptake of the delivery system while other groups are currently evaluating uptake of delivery systems with model drugs such as insulin. We hope that our work may give inspiration to continue the research in that direction.

Acknowledgments

All animal work was conducted in accordance with the Animal Welfare Act, the NIH Guide for the Care and Use of Laboratory Animals, applicable federal and state laws and regulations and the policies of Brown University regarding the care and use of laboratory animals. Dr. Mathiowitz discloses that she is a founder of Perosphere, Inc. and Sentient Bioscience, Inc. It should be noted that the first two authors (Joshua Reineke and Daniel Cho) contributed equally to this work.

Appendix A. Supplementary data

Supplementary data to this article can be found online at http://dx.doi.org/10.1016/j.jconrel.2013.05.043.

References

[1] K. Park, J.R. Robinson, Bioadhesive polymers as platforms for oral-controlled drug delivery: method to study bioadhesion, Int. J. Pharm. 19 (1984) 107–127.
[2] E. Mathiowitz, D. Chickering, J.S. Jacob, C. Santos, Bioadhesive Drug Delivery Systems, in: E. Mathiowitz (Ed.), Encyclopedia of Controlled Drug Delivery, 1st ed. John Wiley & Sons, Inc., New York, NY, 1999, pp. 9–945.
[3] M. Szycher, High Performance Biomaterials, CRC, 1991.
[4] Y. Huang, W. Leobandung, A. Foss, N.A. Peppas, Molecular aspects of muco- and bioadhesion: tethered structures and site-specific surfaces, J. Control. Release 65 (2000) 63–71.
[5] G. Ponchel, J.M. Irache, Specific and non-specific bioadhesive particulate systems for oral delivery to the gastrointestinal tract, Adv. Drug Deliv. Rev. 34 (1998) 191–219.
[6] M.A. Longer, H.S. Ch'ng, J.R. Robinson, Bioadhesive polymers as platforms for oral controlled drug delivery III: oral delivery of chlorothiazide using a bioadhesive polymer, J. Pharm. Sci. 74 (1985) 406–411.
[7] N.A. Peppas, J.J. Sahlin, Hydrogels as mucoadhesive and bioadhesive materials: a review, Biomaterials 17 (1996) 1553–1561.
[8] S. Tamburic, D.Q.M. Craig, A comparison of different *in vitro* methods for measuring mucoadhesive performance, Eur. J. Pharm. Biopharm. 44 (1997) 159–167.
[9] N.A. Peppas, P.A. Buri, Surface, interfacial and molecular aspects of polymer bioadhesion on soft tissues, J. Control. Release 2 (1985) 257–275.
[10] F. Madsen, K. Eberth, J.D. Smart, A rheological examination of the mucoadhesive/mucus interaction: the effect of mucoadhesive type and concentration, J. Control. Release 50 (1998) 167–178.
[11] S.-H.S. Leung, J.R. Robinson, The contribution of anionic polymer structural features to mucoadhesion, J. Control. Release 5 (1988) 223–231.
[12] D. Chickering, J. Jacob, E. Mathiowitz, Poly(fumaric-co-sebacic) microspheres as oral drug delivery systems, Biotechnol. Bioeng. 52 (1996) 96–101.
[13] C.M. Lehr, J.A. Bouwstra, W. Kok, A.B. Noach, A.G. de Boer, H.E. Junginger, Bioadhesion by means of specific binding of tomato lectin, Pharm. Res. 9 (1992) 547–553.
[14] D. Norris, N. Puri, P. Sinko, The effect of physical barriers and properties on the oral absorption of particulates, Adv. Drug Deliv. Rev. 34 (1998) 135–154.
[15] L.A. Kotkoskie, M.T. Butt, E. Selinger, C. Freeman, M.L. Weiner, Qualitative investigation of uptake of fine particle size microcrystalline cellulose following oral administration in rats, J. Anat. 189 (Pt 3) (1996) 531–535.
[16] E. Mathiowitz, J.S. Jacob, Y.S. Jong, G.P. Carino, D.E. Chickering, P. Chaturvedi, et al., Biologically erodable microspheres as potential oral drug delivery systems, Nature 386 (1997) 410–414.
[17] C.A. Santos, J.S. Jacob, B.A. Hertzog, B.D. Freedman, D.L. Press, P. Harnpicharnchai, et al., Correlation of two bioadhesion assays: the everted sac technique and the CAHN microbalance, J. Control. Release 61 (1999) 113–122.
[18] B. Laulicht, P. Cheifetz, A. Tripathi, E. Mathiowitz, Are *in vivo* gastric bioadhesive forces accurately reflected by *in vitro* experiments? J. Control. Release 134 (2009) 103–110.
[19] D.E. Chickering, W.P. Harris, E. Mathiowitz, A microtensiometer for the analysis of bioadhesive microspheres, Biomed. Instrum. Technol. 29 (1995) 501–512.
[20] B. Laulicht, A. Mancini, N. Geman, D. Cho, K. Estrellas, S. Furtado, et al., Bioinspired bioadhesive polymers: dopa-modified poly(acrylic acid) derivatives, Macromol. Biosci. 12 (2012) 1555–1565.
[21] G.P. Carino, J.S. Jacob, C.J. Chen, C.A. Santos, B.A. Hertzog, E. Mathiowitz, Bioadhesive, bioerodible polymers for increased intestinal uptake, in: E. Mathiowitz, D. Chickering, C.-M. Lehr (Eds.), Bioadhesive Drug Delivery Systems: Fundamentals, Novel Approaches, and Development, Marcel Dekker, Inc., 1999
[22] D. Chickering, E. Mathiowitz, Bioadhesive microspheres: I. A novel electrobalance-based method to study adhesive interactions between individual microspheres and intestinal mucosa, J. Control. Release 34 (1995) 251–261.
[23] D.E. Chickering III, J.S. Jacob, E. Mathiowitz, Bioadhesive microspheres, II. Characterization and evaluation of bioadhesion involving hard, bioerodible polymers and soft tissue, React. Polym. 25 (1995) 189–206.
[24] C.G. Thanos, K.P. Yip, E. Mathiowitz, Intestinal uptake of polymer microspheres in the rabbit studied with confocal microscopy, J. Bioact. Compat. Polym. 19 (2004) 247–266.
[25] D.E. Chickering III, J.S. Jacob, T.A. Desai, M. Harrison, W.P. Harris, C.N. Morrell, et al., Bioadhesive microspheres: III. An *in vivo* transit and bioavailability study of drug-loaded alginate and poly(fumaric-co-sebacic anhydride) microspheres, J. Control. Release 48 (1997) 35–46.
[26] C.G. Thanos, Z. Liu, M. Goddard, J. Reineke, N. Bailey, M. Cross, et al., Enhancing the oral bioavailability of the poorly soluble drug dicumarol with a bioadhesive polymer, J. Pharm. Sci. 92 (2003) 1677–1689.
[27] J.S. Jacob, E. Mathiowitz, A novel mechanism for spontaneous encapsulation of active agents: phase inversion nanoencapsulation, ACS Symposium Series CY, American Chemical Society, Washington, DC, 2011, (214–223–223).

[28] G. Ponchel, F. Touchard, D. Duchêne, N.A. Peppas, Bioadhesive analysis of controlled-release systems. I. Fracture and interpenetration analysis in poly(acrylic acid)-containing systems, J. Control. Release 5 (1987) 129–141.
[29] N.A. Peppas, Hydrogels in Medicine and Pharmacy, CRC Press, Boca Raton, FL, 1987.
[30] J. Vasir, Bioadhesive microspheres as a controlled drug delivery system, Int. J. Pharm. 255 (2003) 13–32.
[31] S. Sakuma, R. Sudo, N. Suzuki, H. Kikuchi, M. Akashi, Y. Ishida, et al., Behavior of mucoadhesive nanoparticles having hydrophilic polymeric chains in the intestine, J. Control. Release 81 (2002) 281–290.
[32] G.P. Carino, J.S. Jacob, E. Mathiowitz, Nanosphere based oral insulin delivery, J. Control. Release 65 (2000) 261–269.
[33] P. Arbós, M.A. Campanero, M.A. Arangoa, M.J. Renedo, J.M. Irache, Influence of the surface characteristics of PVM/MA nanoparticles on their bioadhesive properties, J. Control. Release 89 (2003) 19–30.
[34] B. Kriwet, E. Walter, T. Kissel, Synthesis of bioadhesive poly(acrylic acid) nano- and microparticles using an inverse emulsion polymerization method for the entrapment of hydrophilic drug candidates, J. Control. Release 56 (1998) 149–158.
[35] M.A. Jepson, N.L. Simmons, D.T. O'Hagan, B.H. Hirst, Comparison of poly(DL-lactide-co-glycolide) and polystyrene microsphere targeting to intestinal M cells, J. Drug Target. 1 (1993) 245–249.
[36] C. Porta, P. James, A. Phillips, Confocal analysis of fluorescent bead uptake by mouse Peyer's patch follicle-associated M cells, Exp. Physiol. 77 (1992) 929–932.
[37] N. Hussain, V. Jaitley, A.T. Florence, Recent advances in the understanding of uptake of microparticulates across the gastrointestinal lymphatics, Adv. Drug Deliv. Rev. 50 (2001) 107–142.
[38] A. Florence, A. Hillery, N. Hussain, Nanoparticles as carriers for oral peptide absorption: studies on particle uptake and fate, J. Control. Release 36 (1995) 39–46.
[39] P. Jani, G.W. Halbert, J. Langridge, A.T. Florence, The uptake and translocation of latex nanospheres and microspheres after oral administration to rats, J. Pharm. Pharmacol. 41 (1989) 809–812.
[40] A. des Rieux, V. Fievez, M. Garinot, Y.-J. Schneider, V. Préat, Nanoparticles as potential oral delivery systems of proteins and vaccines: a mechanistic approach, J. Control. Release 116 (2006) 1–27.
[41] C. Santos, Evaluation of anhydride oligomers within polymer microsphere blends and their impact on bioadhesion and drug delivery *in vitro*, Biomaterials 24 (2003) 3571–3583.
[42] S.A. Kulkarni, S.-S. Feng, Effects of particle size and surface modification on cellular uptake and biodistribution of polymeric nanoparticles for drug delivery, Pharm. Res. (2013), (Epub ahead of print).
[43] C. He, L. Yin, C. Tang, C. Yin, Size-dependent absorption mechanism of polymeric nanoparticles for oral delivery of protein drugs, Biomaterials 33 (2012) 8569–8578.